0022-3565/00/2951-0352$03.00/0
THE JOURNAL OF PHARMACOLOGY AND EXPERIMENTAL THERAPEUTICS
Vol. 295, No. 1
2735/851329
Printed in U.S.A.

JPET 295:352–359, 2000

Modeling of the In Vivo Antinociceptive Interaction between an Opioid Agonist, (+)-*O*-Desmethyltramadol, and a Monoamine Reuptake Inhibitor, (−)-*O*-Desmethyltramadol, in Rats[1]

MARÍA J. GARRIDO,[2] MARTA VALLE,[3] MIGUEL A. CAMPANERO, ROSARIO CALVO, and IÑAKI F. TROCÓNIZ

Department of Pharmacology, Faculty of Medicine, University of the Basque Country, Bilbao (M.J.G., M.V., R.C.); Department of Clinical Pharmacology, University Hospital, Pamplona (M.A.C.); and Department of Pharmacy and Pharmaceutical Technology, Faculty of Pharmacy, University of Navarra, Pamplona, Spain (I.F.T.)

Accepted for publication June 21, 2000 This paper is available online at http://www.jpet.org

ABSTRACT

The pharmacokinetic-pharmacodynamic (pk-pd) characterization of the in vivo antinociceptive interaction between (+)-*O*-desmethyltramadol [(+)-M1] and (−)-*O*-desmethyltramadol [(−)-M1], main metabolites of tramadol, was studied in three groups of rats. (+)-M1 and (−)-M1, both with different pd properties, were studied under steady-state and nonsteady-state conditions, depending on the group. Plasma drug concentration and antinociception were simultaneously measured in each animal by using an enantioselective analytical assay and the tail-flick test, respectively. Respiratory depression also was evaluated in another series of experiments according to the same experimental conditions. The pk behavior was similar for both enantiomers and no significant ($P > .05$) interaction between two compounds was found at this level. However, a significant ($P < .01$) potentiation in the antinociceptive effect elicited by (+)-M1 was found during and after (−)-M1 administration. The pd model used to describe the time course of the antinociception in the presence of (+)-M1, (−)-M1, or both is based on previous knowledge of the compounds and includes the following: 1) an effect compartment model to account for the opioid effect of (+)-M1, and 2) an indirect response model accounting for the release of noradrenaline (NA) caused by (+)-M1, and the inhibition of the NA reuptake due to the action of (−)-M1. The model predicts a positive contribution to antinociception of the predicted increasing levels of NA. No significant ($P > .05$) respiratory effects were seen during or after (+)-M1 and (−)-M1 administration.

Tramadol is a safe and effective analgesic used in the management of pain and has recently been included in the group of μ-receptor partial agonists, which includes meptazinol (Bowdle, 1998). Results carried out in rats showed that its potency is comparable to that of codeine or dextropropoxiphene (Hennies et al., 1988). However, experimental data suggest that tramadol exerts part of its analgesic effect through the activation of the central inhibitory monoaminergic pathway because its effect has been partially blocked by α_2-adrenoceptor antagonists such as yohimbine (Raffa et al., 1992; Sevcik et al., 1993). The ability of tramadol to inhibit the neuronal uptake of monoamines in the same concentration range at which it binds to μ-opioid receptors, which is very different for morphine or codeine, makes tramadol an "atypical" opioid (Raffa and Friderichs, 1996). The coexistence of opioid and nonopioid mechanisms has been shown in several in vitro and in vivo studies (Hennies et al., 1988; Driessen et al., 1993; Sevcik et al., 1993; Frink et al., 1996; Raffa and Friderichs, 1996; Bamigbade et al., 1997).

Tramadol is a racemic (1:1) mixture of two enantiomers, (+)-tramadol and (−)-tramadol, which are essentially metabolized by the liver (Lee et al., 1993) forming mainly (+)-*O*-desmethyltramadol [(+)-M1] and (−)-*O*-desmethyltramadol [(−)-M1] metabolites, respectively. In vitro studies have shown that the (+)-enantiomers had greater affinity for the opioid receptor system than the (−)-enantiomers, with (+)-M1 being the compound with the highest affinity for μ-receptors (Frink et al., 1996; Lai et al., 1996). However, the capacity to inhibit the synaptosomal uptake of norepinephrine is mainly due to its (−)-enantiomers (Raffa et al., 1992; Driessen et al., 1993; Frink et al., 1996).

In vivo studies have demonstrated an analgesic action of

Received for publication March 23, 2000.
[1] This work was supported by a postdoctoral grant (to M.J.G.) from the Government of Basque Country, Spain.
[2] Current address: Department of Pharmacy and Pharmaceutical Technology, Faculty of Pharmacy, University of Navarra, Pamplona 31080, Spain.
[3] Current address: Department of Biopharmaceutical Sciences, School of Pharmacy, University of California, San Francisco, CA 94143.

ABBREVIATIONS: (+)-M1, (+)-*O*-desmethyltramadol; (−)-M1, (−)-*O*-desmethyltramadol; pk-pd, pharmacokinetic-pharmacodynamic; NA, noradrenaline; Cl, plasma clearance; *Ce*, concentrations in the biophase; k_{e0}, first order rate constant governing the distribution from plasma to biophase; K_{IN}, first order rate constant of release of NA; K_{OUT}, first order rate constant of reuptake of NA.

tramadol in different animal models. This effect was not completely abolished by the administration of naloxone, an opiate antagonist, as occurs with morphine (Hennies et al., 1988; Kayser et al., 1992; Raffa et al., 1993; Bian et al., 1996; Desmeules et al., 1996). These results support the coexistence of dual analgesic mechanisms due to the interaction between the enantiomers of tramadol (Raffa et al., 1995). The action of the opioid system is potentiated by the reinforcement of noradrenergic neurotransmission, especially on spinal neurons (Fairbanks and Wilcox, 1999).

Although these types of interactions have been identified and described in several in vivo studies (Raffa et al., 1993), most of these focus on dose-response relationships. To our knowledge there has so far been no attempt to propose a pharmacokinetic-pharmacodynamic (pk-pd) model capable of describing and predicting the in vivo time course of antinociception when an agonist-opioid and a noradrenaline (NA) uptake blocker are concomitantly administered. Therefore, the aim of the present study was to investigate the in vivo interaction between the enantiomers of M1 in the antinociceptive response by using a mechanism-based pk-pd model. We have recently shown in our laboratory that the in vivo antinociceptive response elicited by (+)-M1 in the tail-flick test could be adequately described by an appropriate pk-pd model (Valle et al., 2000).

Materials and Methods

Animals and Surgery

Male Sprague-Dawley rats with a body weight between 210 and 245 g were used in the experiments. These animals were kept on a controlled light/dark cycle (8:00 AM to 8:00 PM), with a constant temperature of 20°C and humidity of 70°C for a week before experiments were performed. Food (Standard Laboratory Rat, Mouse, and Hamster diets; Panlab, Barcelona, Spain) and water were available ad libitum.

One day before the experiments, the animals were housed individually in plastic cages and three permanent cannulas were implanted under light ether anesthesia: one in the left femoral artery (0.3 mm i.d., 20 cm long; Vygon, Ecouen, France), used for blood sample collection, and two in the right jugular vein (0.5 mm i.d., 10 cm long; Vygon) for (+)-M1 and (−)-M1 administration. All cannulas were filled with a physiological saline solution containing heparin (20 I.U./ml) to prevent clotting. The cannulas were tunneled under the skin and externalized on the dorsal surface of the neck. The protocol of the study was approved by the Committee on Animal Experimentation of the University of the Basque Country.

Pk-Pd Experiments

Three groups of five or six animals each were randomly assigned to different drug treatments. The experiments were always started between 8:30 and 9:00 AM. Each group received (+)-M1 and (−)-M1 according to the protocol summarized in Fig. 1.

Experiment I. (+)-M1 was administered to the animals from group I according to a Wagner infusion scheme calculated to reach rapidly a steady-state plasma concentration of 200 ng ml^{-1} (Wagner, 1974). The animals received an i.v. bolus of 0.73 mg kg^{-1} and immediately afterward, a 160-min continuous i.v. infusion at a rate of 0.023 mg kg^{-1} min^{-1}. Animals received 10-min i.v. infusion of (−)-M1 at a rate of 0.2 mg kg^{-1} min^{-1} starting 120 min after the beginning of the experiment.

Experiment II. Group II received a 10-min i.v. infusion of (+)-M1 at a rate of 0.2 mg kg^{-1} min^{-1} and another 10-min i.v. infusion of (−)-M1 starting 40 min after the beginning of the experiment at a rate of 0.2 mg $kg^{-1}min^{-1}$.

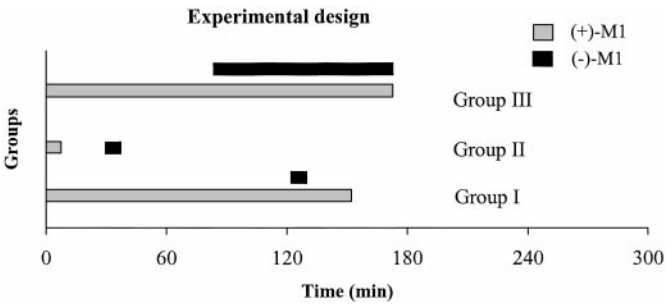

Fig. 1. Experimental design for (+)-M1 and (−)-M1 administration in each of the three groups of the study. The length of different infusions is represented by solid bars: ▨, (+)-M1; and ■, (−)-M1.

Experiment III. The animals from group III received two i.v. infusions according to the Wagner infusion scheme for both compounds, to reach rapidly a steady-state plasma concentration of 200 ng ml^{-1} for (+)-M1 and 500 ng ml^{-1} for (−)-M1. The first compound was administered as an i.v. bolus of 0.73 mg kg^{-1}, and immediately afterward a 180-min continuous i.v. infusion was given at a rate of 0.023 mg kg^{-1} min^{-1}. The second compound was administered at 90 min after the start of the experiment as an i.v. bolus of 2.55 mg kg^{-1} followed by a 90-min continuous i.v. infusion at a rate of 0.068 mg kg^{-1} min^{-1}.

To determine the pk of (+)-M1 and (−)-M1, several blood samples (125–225 μl) were collected at fixed intervals over the time course of the experiments. Blood samples were centrifuged at 2500 rpm for 15 min and the plasma was stored at −20°C until HPLC analysis (see below).

The antinociception for the three above-mentioned groups was simultaneously evaluated at the same time as blood samples were collected. This effect was measured by the radiant-heat tail-flick technique to assess the nociception threshold (D'Amour and Smith, 1941). Tail-flick latency was measured automatically with a Letica analgesimeter (Letica, Barcelona, Spain). The intensity of heat was adjusted so that baseline latencies were between 2 or 3 s; animals with higher baseline latencies were excluded from the study. A maximum cutoff time of 10 s was used to prevent tissue damage. Three extra (control) groups that received physiological saline solution at different rates according to the protocols previously described were used to evaluate the effect of the length of infusion and repeated tail-flick measurements in the time course of antinociception.

Respiratory Depression

Experiment IV. Twelve animals were randomly divided into four groups to study the possible interaction between (+)-M1 and (−)-M1 on the respiratory depression. These compounds were concomitantly administered according to the same scheme of the infusions as described above (Fig. 1). Additionally, an extra group (control group) received a physiological saline solution for 180 min to evaluate the effect of the length of the infusion on the pH, pCO_2, and pO_2 basal levels. Several arterial blood samples (100 μl) were collected before, during, and after infusions to measure the pH, pCO_2, and pO_2 levels by a gas analyzer (AVL 990; AVL Biomedical Instruments, Graz, Austria).

Drug Assay

The plasma concentrations of (+)-M1 and (−)-M1 were determined by a sensitive and stereoselective HPLC assay (Campanero et al., 1999). Briefly, plasma samples (50–100 μl) were transferred into glass tubes mixed with 50 μl of internal standard (ketamine HCl), 1 ml of Tris buffer (pH 9.5, 0.05 M), and 6 ml of *tert*-butyl methylether. The mixture was shaken for 1 min and the organic layer was separated after centrifugation at 3500 rpm for 10 min. The organic phase was evaporated to dryness at 40°C under reduced pressure (rotatory evaporator, model 4322000; Labconco, Kansas City, MO). The resi-

due was reconstituted in 250 μl of mobile phase and vortex mixed for 1 min. A 100-μl aliquot was then injected into the HPLC system.

The chromatography system consisted of a Hewlett Packard HPLC (Waldbronn, Germany) equipped with an HP 1050 quaternary pump, an HP 1050 autosampler, and an HP 1046A fluorescence detector. The excitation and emission λ were 199 and 301 nm, respectively.

The analytical separation was performed at 20 ± 3°C by a Chiralcel OD-R column (250 × 4.6 mm i.d.) packed with cellulose Tris (3,5-dimethylphenylcarbamate) coated in silica (10 μm) (Daicel Chemical Industries, Tokyo, Japan), preceded by a reversed phase, 100 × 4-mm end-capped column packed with 3 μm of C8 silica reversed phase particles (Hypersil BDS C18; Hewlett Packard). A guard column (4 × 4 mm) packed with Lichrosphere 100 DIOL (5 μm) from Merck (Barcelona, Spain) was connected to the column system. The mobile phase consisting of acetonitrile plus 0.05 M sodium dihydrogen phosphate, thiethylamine (0.09 M), and sodium perchlorate (0.2 M), adjusted to pH 5.5 with hydrochloric acid 2 M (20 acetonitrile/80 buffer, pH 5.5), was filtered through a 0.45-μm pore size membrane filter. The flow rate was 0.6 ml min^{-1}. The limit of quantification of each enantiomer was 10 ng ml^{-1} and the method was linear from 10 to 1000 ng ml^{-1}. The intra- and interassay coefficients of variation were 2.8 and 4.9%, respectively.

Data Analysis

All the analysis was performed by using the population approach with NONMEM V (Beal and Sheiner, 1992). During the analysis the pk model was built first and then, with all parameters of the pk model fixed, the pd model was elaborated. The observations are expressed as follows: $OBS_{ij} = f(\theta_i, D, t_j) + \epsilon_{ij}$, where OBS_{ij} refers to the jth observation (plasma drug concentration, or antinociceptive effect), obtained at time t_j in the ith animal; f represents the structural model; θ_i represents the set of the parameters (pk or pd) for the ith animal; D is the administered dose, and ϵ_{ij} represents the residual shift of the observation from the model predictions. ϵ_{ij} are random variables assumed to be symmetrically distributed around zero with variance denoted by σ^2. Although in the previous expression an additive model was used to relate observations to predictions, different error models were tested.

For each of the elements of θ_i, the following model was used: $p_i = p_{pop} \cdot \exp(\eta_i)$, where p_i represents an arbitrary pk or pd parameter of the ith animal; p_{pop} is the mean population estimate, and η_i, the shift of the parameter of the ith animal from the population mean estimate, are random variables assumed to be symmetrically distributed around zero with variance-covariance matrix Ω with diagonal elements $(\omega^2_1, \ldots, \omega^2_m)$, m being the number of pk or pd parameters estimated in the model.

Pk Models. The disposition of the drug in the body was characterized by compartmental models. Distribution and elimination of (−)-M1 were modeled as linear processes. However, as has been described before for (+)-M1 (Valle et al., 2000), the plasma clearance (Cl) was described as a function depending on the time after the start of the infusion as follows: $Cl = Cl_1 \cdot \exp(-Cl_2 \cdot t)$; Cl_1 and Cl_2 are pk parameters to be estimated by the model and t represents time after the start of the infusion.

Pd Models. The pd model accounting for the in vivo interaction between (+)-M1 and (−)-M1 on the antinociceptive effect is represented in Fig. 2. It consists of three submodels, which were based on the following considerations.

Submodel 1. An effect compartment model (Sheiner et al., 1979) has been shown to be adequate to account for the disequilibrium between plasma and biophase concentrations of (+)-M1 (Valle et al., 2000). In Fig. 2, k_{e0} is the first order rate constant governing the distribution of (+)-M1 from plasma to biophase.

Submodel 2. The administration of opioid drugs results in a concomitant release of NA, and there is evidence that such a release may contribute to the antinociceptive effect of the opioid (Bouaziz et al., 1996). In Fig. 2, K_{IN} and K_{OUT} represent the first order rate constants of release and reuptake of NA, respectively.

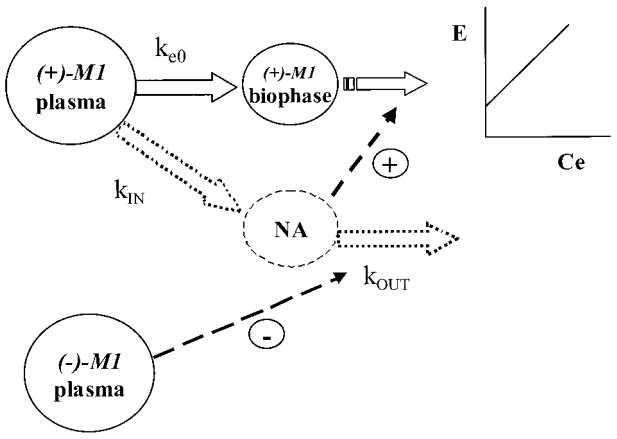

Fig. 2. Schematic representation of the pd model selected during the analysis of the in vivo interaction between (+)-M1 and (−)-M1 in the antinociceptive effect.

In the absence of (−)-M1, the rate of change of NA is represented by the following expression:

$$\frac{dNA}{dt} = K_{IN} \cdot C_{(+)\text{-M1}} - K_{OUT} \cdot NA\,, \qquad (1)$$

where $C_{(+)\text{-M1}}$ is the plasma concentrations of (+)-M1.

Submodel 3. (−)-M1 is able to inhibit the reuptake of NA (Raffa et al., 1992; Driessen et al., 1993; Frink et al., 1996). In the presence of (−)-M1 the rate of change of NA is described by the following expression:

$$\frac{dNA}{dt} = K_{IN} \cdot C_{(+)\text{-M1}} - K_{OUT} \cdot I(t) \cdot NA\,, \qquad (2)$$

where $I(t) = (1 - SL_2 \cdot C_{(-)\text{-M1}})$; $C_{(-)\text{-M1}}$ is the plasma concentration of (−)-M1 and SL_2 is the slope of the linear relationship between K_{OUT} and $C_{(-)\text{-M1}}$.

The final interaction model has the following expression: Antinociception $= E_0 + SL \cdot Ce_{(+)\text{-M1}} \cdot (1 + NA)$, where E_0 represents the baseline latency and SL the slope of the linear relationship between the antinociceptive effect elicited by the opioid system and the effect site (+)-M1 concentrations, $Ce_{(+)\text{-M1}}$. The model predicts no effect of the (−)-M1 enantiomer when it is administered alone, and assumes that the plasma concentrations of (+)-M1 and (−)-M1 are the ones directly related to the release and inhibition of the reuptake of NA, respectively. Alternative models assuming 1) an effect compartment for the effect of (−)-M1; 2) $Ce_{(+)\text{-M1}}$ instead of $C_{(+)\text{-M1}}$ is directly related with NA release; or 3) effect versus concentrations can be better described by an E_{max} or sigmoidal E_{max} models also were fitted to the data. In addition, a model ignoring the contribution of (−)-M1 to the antinociceptive effect was explored.

Model selection was based on a number of criteria, such as the exploratory analysis of the goodness of fit plots, the estimates and the confidence intervals of the fixed and random parameters, and the minimum value of the objective function provided by NONMEM; the difference in the objective function between two hierarchical models was compared with a chi-square distribution in which a difference of approximately 4, 6, and 11 points was significant at the 5, 1, and 0.1% levels, respectively.

Statistical Analysis

The paired Student's t test (two-tailed) was used for comparison between the maximum effects after (+)-M1 administration and after (−)-M1 administration. To evaluate the respiratory depression in all

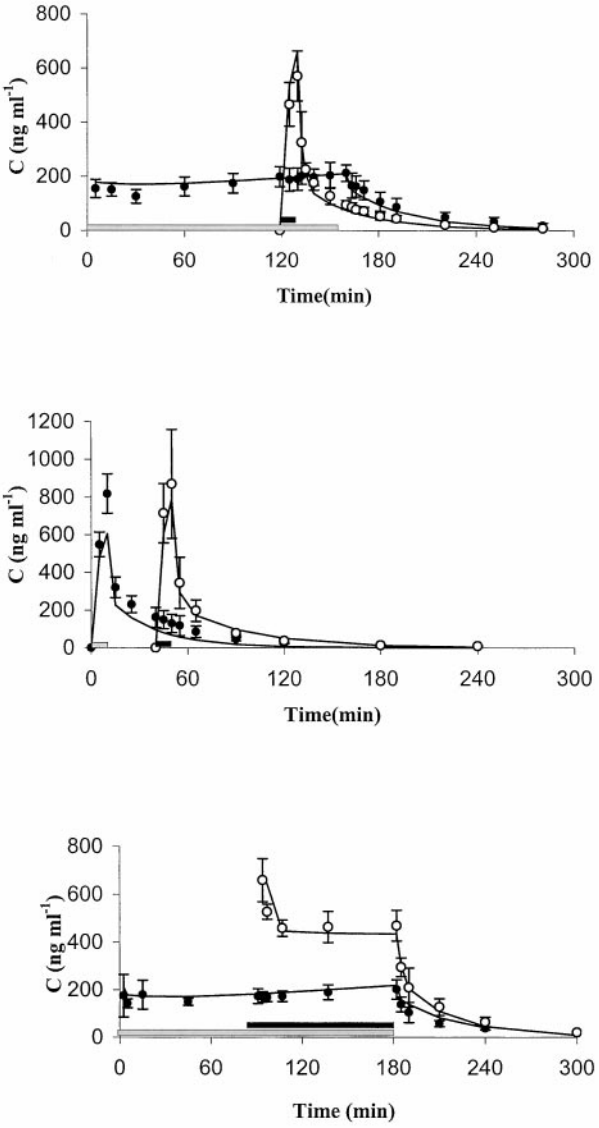

Fig. 3. Pk profiles of (+)-M1 (●) and (−)-M1 (○) in group I (top), II (middle), and III (bottom). The points represent the mean observed concentrations, the solid lines the typical model predictions, and the vertical lines are the standard deviations. The solid bars represent the length of different infusions: ▨, (+)-M1; and ■, (−)-M1.

groups an ANOVA followed by the F test was used. A probability level of $P < .05$ was considered to be statistically significant.

Compounds

The hydrochloride salts of (+)-M1 and (−)-M1 were kindly supplied by Grünenthal GmbH (Aachen, Germany). Ketamine HCl (internal standard) was purchased from Sigma Chemical Co. (Madrid, Spain). All reagents and solvents were of analytical grade.

Results

Pk of (+)-M1 and (−)-M1. Figure 3 shows the mean observed plasma concentrations versus time profiles for both enantiomers over the time course of the experiment. The infusion design produced a rapid steady state in plasma for (+)-M1 in groups I and III, and for (−)-M1 in group III.

Figure 3 also represents the typical model predictions. The selected model for both enantiomers was a two-compartment model. For (+)-M1 total Cl was modeled as a function dependent on the time after the start of the infusions. Estimates of the fixed and random parameters for (+)-M1 are listed in Table 1. Interanimal variability could be estimated in total Cl and apparent volume of distribution of the peripheral compartment (V_T) resulting in 37 and 30%, respectively.

Estimates of the pk parameters for (−)-M1 are listed in Table 2. Their values were very similar to that obtained for (+)-M1, the main difference being the fact that Cl was constant over time. Interanimal variability could be estimated in total Cl, intercompartmental clearance (Cl_d), and in the apparent volume of the V_T. The variability in the total clearance (15%) was low in comparison to the 50 and 30% estimates obtained for Cl_d and V_T, respectively. Residual variability was less than 10% for both (+)-M1 and (−)-M1.

Different models testing the possible effect of the plasma concentrations of (+)-M1 on the value of the pk parameters of (−)-M1, and vice versa also were fitted, however, no improvements were found in respect to the model showed in Fig. 3.

Pk-Pd Results. The mean observed antinociceptive effect versus time profiles for the three groups are shown in Fig. 4. The antinociceptive baseline values did not significantly ($P > .05$) differ between groups. At the time of the start of (−)-M1 administration, the observed mean antinociceptive effect elicited by (+)-M1 was 7.6 ± 0.5, 8.3 ± 0.7, and 5.1 ± 0.3 s in groups I, II, and III, respectively. These values were significantly increased ($P < .05$) to values of 10 s for group I and 8.6 ± 1.7 s for group III, at the times the infusion of (−)-M1 was stopped. However, the increase to 9.3 ± 1.4 s in group II was not statistically significant; but, it should be taken into account that for group II, at times the infusion of (−)-M1 was started, plasma concentrations of (+)-M1 were already decreasing. In groups I and III mean plasma (+)-M1 concentrations remained constant during the (−)-M1 infusion (Fig. 3). These results suggested an enhancement in the antinociception due to the presence of (−)-M1. Peak effect after (−)-M1 administration was observed at 130, 50, and from 120 to 180 min for group I–III, respectively. No significant differences ($P > .05$) from the basal latency values throughout the period of the experiment were found in each of the extra control groups.

Figure 4 also shows the typical predictions for two of the models tested: the simplest model (an effect compartment model), not including drug interaction and assuming that all the effect is caused by (+)-M1 action; and the final selected model, including the inhibition of the NA reuptake by (−)-M1 action. This last model was capable of describing the effect of (+)-M1 and also the increase in observed antinociception immediately after (−)-M1 administration, in the three

TABLE 1
Pharmacokinetic parameter estimates of (+)-M1
Estimates of interanimal variability are expressed as coefficients of variation (%). Precision of the estimates is expressed as relative standard error in parenthesis. Relative standard error is standard error divided by the parameter estimate.

Parameter	Estimate	Interanimal Variability
V_c(l)	0.066 (0.57)	N.E.
V_T(l)	0.590 (0.06)	30 (0.66)
Cl_d (l min^{-1})	0.075 (0.11)	N.E.
Cl_1 (l min^{-1})	0.034 (0.08)	37 (0.54)
Cl_2 (min^{-1})	0.002 (0.36)	

V_c, initial volume of distribution; V_T, apparent volume of distribution of the peripheral compartment; Cl_d, intercompartmental clearance; $Cl = Cl_1 \cdot e^{-Cl_2 \cdot t}$; N.E., not estimated in the model.

TABLE 2

Pharmacokinetic parameter estimates of (−)-M1

Estimates of interanimal variability are expressed as coefficients of variation (%). Precision of the estimates is expressed as relative standard error in parenthesis. Relative standard error is standard error divided by the parameter estimate.

Parameter	Estimate	Interanimal Variability
V_c (l)	0.170 (0.08)	N.E.
V_T (l)	0.563 (0.12)	39 (0.45)
Cl_d (l min^{-1})	0.034 (0.14)	50 (0.46)
Cl (l min^{-1})	0.031 (0.07)	15 (0.36)

V_c, initial volume of distribution; V_T, apparent volume of distribution of the peripheral compartment; Cl_d, intercompartmental clearance; N.E., not estimated in the model.

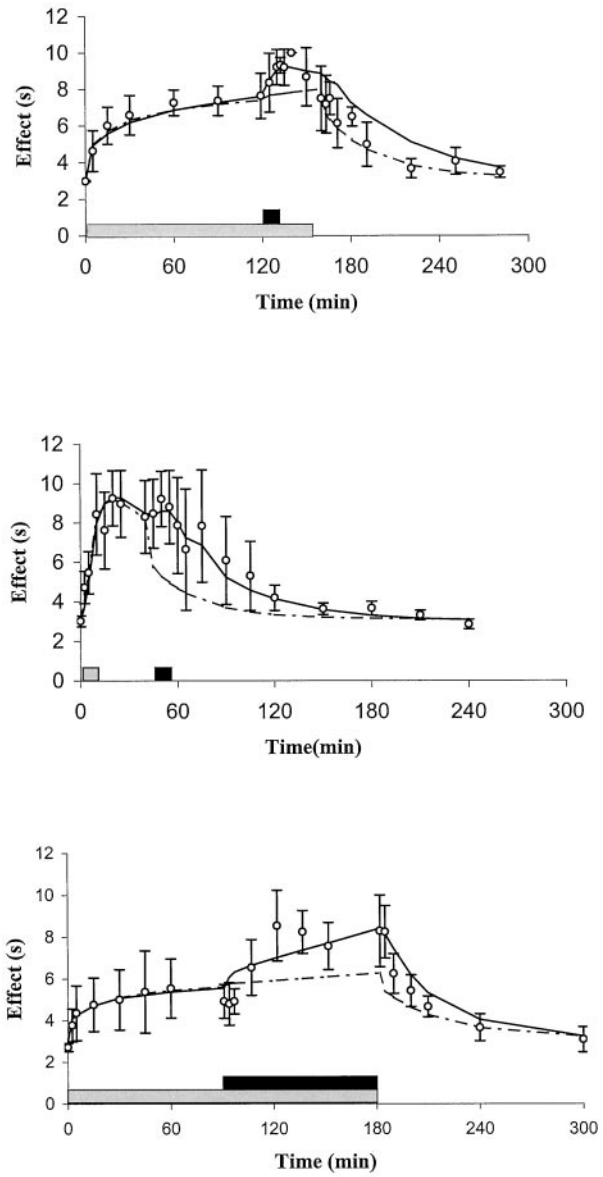

Fig. 4. Time course of antinociception in group I (top), II (middle), and III (bottom). Points represent the mean observed antinociception; dashed lines represent typical predictions from the model, not including interaction between the two enantiomers; and solid lines are the typical predictions from the model described in Fig. 2 (selected model). Horizontal bars represent the time and length of (+)-M1 (▨) and (−)-M1 (■) infusions. Vertical lines are the standard deviations.

groups of animals. Note, at times (−)-M1 infusion was stopped, the 2-fold differences between the mean observed effect and the prediction obtained from the model does not include the (+)-M1-(−)-M1 interaction (Fig. 4, middle). Table 3 lists the estimate of the pd parameters for the final model. Interanimal variability could be estimated in only two parameters, SL and k_{e0}. In the range of concentrations seen in the current study the pd relationships for (+)-M1 and (−)-M1 were found to be linear. Figure 5 represents the predicted time profiles of arbitrary NA levels on the basis of the selected model.

Respiratory Depression Results. Mean observed time profiles for pH, pCO_2, and pO_2 are depicted in Fig. 6. (+)-M1 administration did not elicit significant changes in any of the respiratory parameters ($P > .05$). In addition, despite the increase seen in the antinociceptive effect, the administration of (−)-M1 had no significant implications for the respiratory function ($P > .05$).

Discussion

In this study the in vivo interaction on the antinociceptive effect between the two main metabolites of tramadol, (+)-M1 and (−)-M1, has been characterized by using a pk-pd model. The interaction between opiate drugs and α_2-adrenergic agonists or monoamine reuptake inhibitors has been reported in the literature by several studies. Meert and De Kock (1994) found a potentiation in the effect elicited by opioids when α_2-adrenergic agonists were concomitantly administered. The estimate of ED_{50} for fentanyl in the tail-withdrawal response test when it was given 120 min after xylazine treatment decreased from 0.22 to 0.056 mg kg^{-1} when xylazine doses were increased from 0.63 to 40 mg kg^{-1}, respectively. Similar results were found in the duration of sufentanil analgesia after medetomidine i.v. administration. A 0.063 mg kg^{-1} dose of medetomidine provided a statistical ($P < .05$) increase in the duration of analgesia after an i.v. administration of a 1.25-μg dose of sufentanil. Taiwo et al. (1985) also reported a potentiation of morphine antinociception measured by tail-flick test after tricyclic antidepressant administration. An s.c. dose of 0.5 mg kg^{-1} morphine did not produce any change in the antinociceptive baseline, but when the same s.c. dose was given together with 30 μg of amitriptyline intrathecally, all animals reached maximum response.

There are still questions regarding the time course of the in vivo effect of tramadol such as what is the role of the metabolites, or which kind of interaction occurs between (+)- and (−)-enantiomers. Poulsen et al. (1996) suggested that forma-

TABLE 3

Results from the final population pharmacodynamic model selected

Estimates of interanimal variability are expressed as coefficients of variation (%). Precision of the estimates is expressed as relative standard error in parenthesis. Relative standard error is standard error divided by the parameter estimate.

Parameter	Estimate	Interanimal Variability
E_0 (s)	2.98 (0.04)	N.E.
SL (s ml ng^{-1})	0.0216 (0.11)	19.7 (0.40)
k_{e0} (min^{-1})	0.041 (0.20)	47.9 (1.14)
SL_2 (ml s^{-1} ng^{-1})	0.00211 (0.04)	N.E.
K_{IN} (min^{-1})	0.60E-4 (0.38)	N.E.
K_{OUT} (min^{-1})	0.114 (0.13)	N.E.

E_0, antinociceptive baseline; SL, slope of the linear relationship between the antinociceptive effect elicited by the opioid system and $Ce_{(+)\text{-M1}}$; k_{e0}, first order rate constant of equilibrium between plasma and effect compartment; SL_2, slope of the linear relationship between K_{OUT} and $C_{(-)\text{-M1}}$; K_{IN}, first order rate constant of release of NA; K_{OUT}, first order rate constant of NA reuptake; N.E., not estimated in the model.

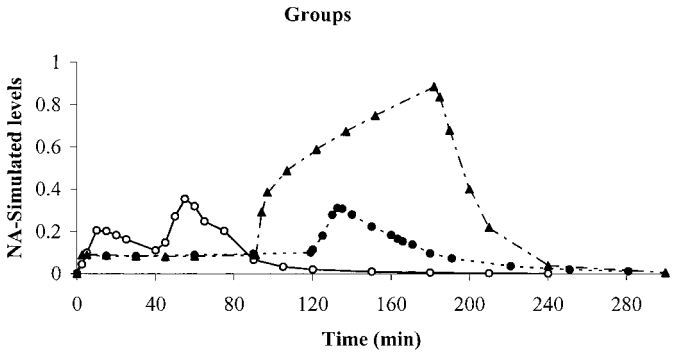

Fig. 5. Predicted arbitrary levels of NA versus time obtained from the selected pd model depicted in Fig. 2 in group I (○), II (●), and III (▲).

tion of (+)-M1 is important for the effect of tramadol. On the basis of these considerations and to make simpler the study of all possible combinations between (+)-tramadol, (+)-M1, (−)-tramadol, and (−)-M1, we focused our study only on the combination of (+)-M1 and (−)-M1. An interaction is "a priori" expected given the opioid and monoamine reuptake inhibition properties of (+)-M1 and (−)-M1, respectively.

Previous studies carried out in our laboratory showed that the in vivo antinociceptive effect of (+)-M1 in rats could be adequately characterized by a pk-pd model (Valle et al., 2000). We also found that high doses of (−)-M1 such as 8 mg kg^{-1} or steady-state plasma concentration levels of 700 ng ml^{-1} did not elicit antinociceptive response. To achieve the goal of this study, results from that pk-pd study were used. Steady-state plasma concentration levels of 200 ng ml^{-1} of (+)-M1 were found to exhibit an antinociceptive response between 50 and 70% of the maximum response expressed as percentage of the baseline. Choosing this target effect level gave enough response window to evaluate the eventual potentiation caused by the (−)-M1 administration and also represented a significant response level with respect to the baseline. The experimental design used in the current study simultaneously explored the in vivo antinociception in three different situations: 1) steady state for (+)-M1 and acute administration of (−)-M1 (group I), 2) acute administration for both compounds (group II), and 3) steady state for both compounds (group III). This design has been determined to be adequate to characterize the in vivo effect in cases where there is delay in the distribution from plasma to biophase, and development of tolerance occurs (Ekblom et al., 1993). In fact, both phenomena were seen in our previous study with (+)-M1 (Valle et al., 2000). The doses given for (−)-M1 were chosen on the basis of the previous pk knowledge. We decided to give first the infusion of (+)-M1 and then infuse the (−)-M1 because this design allowed us to compare the eventual enhancement in antinociception caused by (−)-M1 within each animal in the study, and generate data suitable to develop a pk-pd model describing drug interactions.

Figure 3 shows that the selected dosage regimen produced the target-desired mean-observed concentrations rapidly in groups I and III. In group II this value of concentration was achieved at the time of (−)-M1 administration. The estimates of pk parameters were very similar to those obtained previously when both compounds were administered alone (Valle et al., 2000). These results show that there is no pk interaction between the two enantiomers of the metabolite.

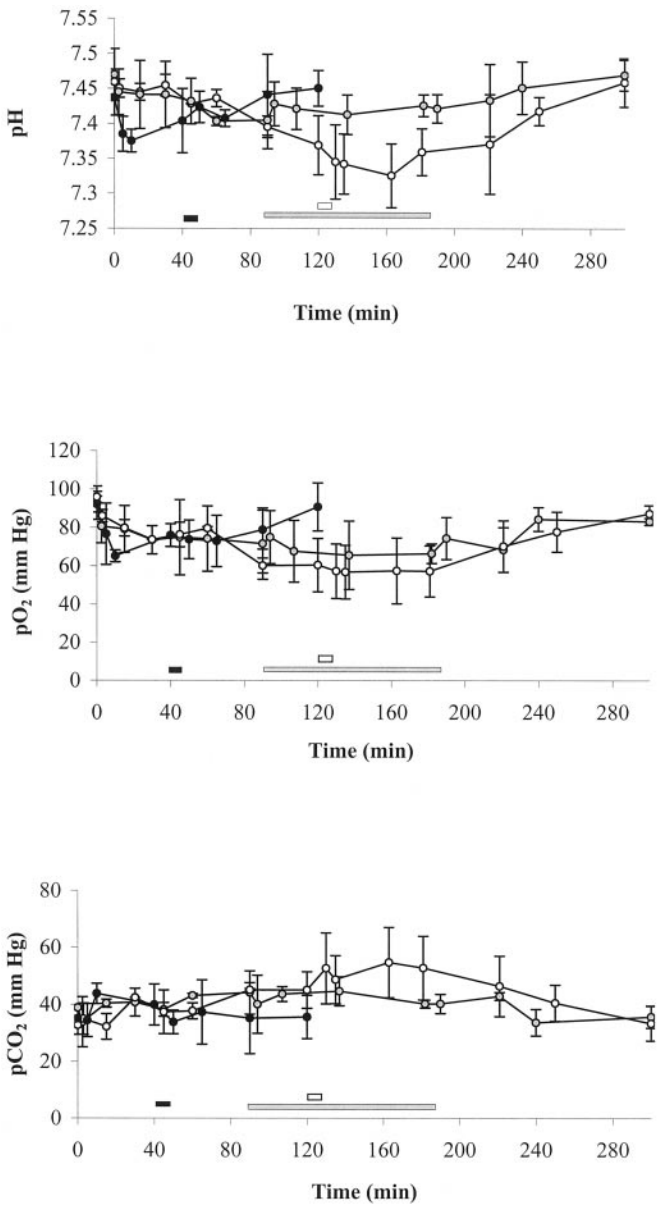

Fig. 6. Mean observed levels of pH (upper panel), pO_2 (middle panel), and pCO_2 (lower panel) in groups receiving (+)-M1 and (−)-M1 in a similar infusion design that has been described in Fig. 1 for group I (○), group II (●), and group III (◍). Horizontal bars represent the time and length of (−)-M1 infusions for group I (□), group II (■), and group III (▤). Vertical lines are the standard deviations.

During the pd analysis in a first step, the observed effect between the start of the experiment and before (−)-M1 administration was related to the predicted (+)-M1 plasma concentration. These analyses showed that there was a significant delay for the drug in plasma to reach the biophase. The estimate of k_{e0} was 0.04 min^{-1} and the slope of the effect versus effect site concentration was estimated at 0.0208 s min^{-1}. These values were very close to those previously reported for (+)-M1 by using completely different dosage designs for this compound. In fact, the target response (50–70% of the maximum response) was achieved by using the results from a previous study (Valle et al., 2000). When the entirely observed effect versus time profiles were related to the plasma concentrations of (+)-M1, the best fit result gave the predictions represented by dashed lines in Fig. 4. It is

clear that this model is unable to describe the response during and after (−)-M1 administration, especially the peak effects. With this model, maximum differences between the observed and model predicted effect were 2.1 s for group I, 4 s for group II, and 2.4 s for group III. From these results it is clear that a pd interaction between (+)-M1 and (−)-M1 has occurred.

More pk-pd modeling is incorporating models accounting for complex mechanisms of action (Gries et al., 1998; Brynne et al., 1999; Gozzi et al., 1999). The model used in the current study to describe the data represents a noncompetitive interaction model that is based on the following proposal mechanism: systemic administration of therapeutic doses of opioids elicits an increase of NA levels in the lumbar cerebrospinal fluid; this spinal-released NA could contribute to analgesia by an indirect stimulation of α_2-adrenoceptors (Bouaziz et al., 1996; Xu et al., 1997; Song et al., 1998). Therefore, the presence of the NA reuptake inhibitor (−)-M1 (Frink et al., 1996) produces an augmentation of synaptic NA in spinal cord, which is responsible for the enhancement in the antinociception elicited by (+)-M1.

This mechanism of action was modeled by using an indirect response model, in which NA levels were released by (+)-M1 and (−)-M1 was acting to inhibit the first order rate constant of elimination of NA levels from the spinal site. Figure 5 shows the arbitrary NA levels simulated as a function of release promoted by (+)-M1 and inhibition of its reuptake caused by (−)-M1. Studies with microdialysis techniques offer the possibility to compare the observed time course of NA and (+)-M1 and (−)-M1 concentrations in the spinal space with the relative model-predicted concentrations of NA and model-predicted drug concentrations obtained in the current study.

The selected model represented by the solid line in Fig. 4, which was able to adequately describe the entire course of the drug effect, predicts no effect when there is no NA release caused by opioid drug, which is compatible with the findings that (−)-M1 has no antinociceptive effect per se. The estimate of K_{OUT} is much higher that that obtained for K_{IN}, suggesting that the contribution of NA to opioid antinociception diminished quickly after release.

Tramadol given at doses higher than 1 mg kg^{-1} i.v. produced respiratory depression in anaesthetized rats (Raffa and Friederichs, 1996). That effect was abolished by previous treatment with an enzyme inhibitor (SKF-525-A), suggesting that the adverse effect was mainly due to the (+)-M1 presence. In previous studies we have seen that doses of (+)-M1 up to 2.5 mg kg^{-1} i.v. did not produce any respiratory effect. In the current study no respiratory depression was found after (+)-M1 or (−)-M1 administration. These results show that (−)-M1 in the range of plasma concentrations obtained for (+)-M1 and (−)-M1 had no influence on the respiratory parameters.

To summarize the results from the current study a pd interaction reflected as a potentiation in the antinociceptive effect was found between two enantiomers of the main active metabolite of tramadol, *O*-desmethyltramadol. This phenomenon has successfully been modeled by using a noncompetitive interaction model based on previous knowledge about the mechanism of action of both compounds.

Acknowledgments

We thank Grünenthal for the generous gifts of (+)-M1 and (−)-M1. We also thank the Research Department of Cruces Hospital (Bizkaia) for giving us the possibility to measure the respiratory depression effect of this study.

References

Bamigbade TA, Davidson C, Langford RM and Stamford JA (1997) Actions of tramadol, its enantiomers and principal metabolite, O-desmethyltramadol, on serotonin (5-HT) efflux and uptake in the rat dorsal raphe nucleus. *Br J Anaesth* **79:**352–356.

Beal SL and Sheiner LB eds (1992) *NONMEM Users Guides*. NONMEM Project Group, University of California at San Francisco, San Francisco.

Bian D, Nichols ML, Ossipov MH and Porreca F (1996) Antiallodynic effects of tramadol on a model of neuropathic pain in rats. *Analgesia* **2:**57–62.

Bouaziz H, Tong CH, Yoon Y, Hood DD and Eisenach JC (1996) Intravenous opioids stimulate norepinephrine and acetylcholine release in spinal cord dorsal horn. Systematic studies in sheep and an observation in a human. *Anesthesiology* **84:** 143–154.

Bowdle TA (1998) Adverse effects of opioid agonists and agonist-antagonists in anaesthesia. *Drug Safety* **19:**173–189.

Brynne L, Paalzow LK and Karlsson MO (1999) Mechanism-based modeling of rebound tachycardia after chronic *l*-propranolol infusion in spontaneous hypertensive rats. *J Pharmacol Exp Ther* **290:**664–671.

Campanero MA, Calahorra B, Valle M, Troconiz IF and Honorato J (1999) Enantiomeric separation of tramadol and its active metabolite in human plasma by chiral high-performance liquid chromatography: Application to pharmacokinetic studies. *Chirality* **11:**272–279.

D'Amour FE and Smith DL (1941) A method for determining loss of pain sensation. *J Pharmacol Exp Ther* **72:**74–79.

Desmeules JA, Piguet V, Collart PL and Dayer P (1996) Contribution of monoaminergic modulation to the analgesic effect of tramadol. *Br J Pharmacol* **41:**7–12.

Driessen B, Reimann W and Giertz H (1993) Effects of the central analgesic tramadol on the uptake and release of noradrenaline and dopamine *in vitro*. *Br J Pharmacol* **108:**806–811.

Ekblom M, Hammarlund-Udenaes M and Paalzow L (1993) Modeling of tolerance development and rebound effect during different intravenous administrations of morphine to rats. *J Pharmacol Exp Ther* **266:**244–252.

Fairbanks CA and Wilcox GL (1999) Spinal antinociceptive synergism between morphine and clonidine persists in mice made acutely or chronically tolerant to morphine. *J Pharmacol Exp Ther* **288:**1107–1116.

Frink MCH, Hennies HH, Englberger W, Haurand M and Wilffert B (1996) Influence of tramadol on neurotransmitter systems of the rat brain. *Arzneim-Forsch/Drug Res* **46:**1029–1036.

Gozzi P, Påhlman I, Palmér L, Grönberg A and Persson S (1999) Pharmacokinetic-pharmacodynamic modeling of the immunomodulating agent susalimod and experimentally induced tumor necrosis factor-α levels in the mouse. *J Pharmacol Exp Ther* **291:**199–203.

Gries JM, Munafo A, Porchet HC and Verotta D (1998) Down-regulation models and modeling of testorone production induced by recombinant human choriogonadotropin. *J Pharmacol Exp Ther* **289:**371–377.

Hennies HH, Friderichs E and Schneider J (1988) Receptor binding, analgesic and antitussive potency of tramadol and other selected opioids. *Arzneim-Forsch/Drug Res* **38:**877–880.

Kayser V, Besson JM and Guilbaud G (1992) Evidence for a noradrenergic component in the antinociceptive effect of the analgesic agent tramadol in an animal model of clinical pain, the arthritic rat. *Eur J Pharmacol* **224:**83–88.

Lai J, Ma S, Porreca F and Raffa RB (1996) Tramadol, M1 metabolite and enantiomer affinities for cloned human opioid receptors expressed in transfected HN9.10 neuroblastoma cells. *Eur J Pharmacol* **316:**369–372.

Lee CR, McTavish D and Sorkin EM (1993) Tramadol. A preliminary review of its pharmacodynamic and pharmacokinetic properties, and therapeutic potential in acute and chronic pain states. *Drugs* **46:**313–340.

Meert TF and De Kock M (1994) Potentiation of the analgesic properties of fentanyl-like opioids with α_2-adrenoceptor agonists in rats. *Anesthesiology* **81:**677–688.

Poulsen L, Arendt-Nielsen L and Sindrup SH (1996) The hypoalgesic effect of tramadol in relation to CYP2D6. *Clin Pharmacol Ther* **60:**636–644.

Raffa RB and Friderichs E (1996) The basic science aspect of tramadol hydrochloride. *Pain Rev* **3:**249–271.

Raffa RB, Friderichs E, Reimann W, Shank RP, Codd EE and Vaught JL (1992) Opioid and nonopioid components independently contribute to the mechanism of action of tramadol, an "atypical" opioid analgesic. *J Pharmacol Exp Ther* **260:**275–285.

Raffa RB, Friderichs E, Reimann W, Shank RP, Codd EE, Vaught JL, Jacoby HI and Selve N (1993) Complementary and synergistic antinociceptive interaction between the enantiomers of tramadol. *J Pharmacol Exp Ther* **267:**331–340.

Raffa RB, Nayak RK, Liao S and Minn FL (1995) The mechanism(s) of action and pharmacokinetics of tramadol hydrochloride. *Rev Contemp Pharmacother* **6:**485–497.

Sevcik J, Nieber K, Driessen B and Illes P (1993) Effects of the central analgesic tramadol and its main metabolite, O-desmethyltramadol, on rat locus coeruleus neurones. *Br J Pharmacol* **110:**169–176.

Sheiner LB, Stanski DR, Vozeh S, Miller RD and Ham J (1979) Simultaneous modelling of pharmacokinetics and pharmacodynamics: Application to d-tubocuranine. *Clin Pharmacol Ther* **25:**358–371.

Song HK, Pan HL and Eisenach JC (1998) Spinal nitric oxide mediates antinociception from intravenous morphine. *Anesthesiology* **89:**215–221.

Taiwo YO, Fabian A, Pazoles CHJ and Fields HL (1985) Potentiation of morphine antinociception by monoamine reuptake inhibitors in the rat spinal cord. *Pain* **21:**329–337.

Valle M, Garrido MJ, Pavón JM, Calvo R and Trocóniz IF (2000) Pharmacokinetic-pharmacodynamic modeling of the antinociceptive effects of main active metabolites of tramadol, (+)-*O*-desmethyltramdol and (−)-*O*-desmethyltramadol, in rats. *J Pharmacol Exp Ther* **293:**646–653.

Wagner JG (1974) A safe method for rapidly achieving plasma concentration plateaus. *Clin Pharmacol Ther* **16:**691–700.

Xu Z, Tong CH, Pan HL, Cerda SE and Eisenach JC (1997) Intravenous morphine increases release of nitric oxide from spinal cord by an α-adrenergic and cholinergic mechanism. *J Neurophysiol* **78:**2072–2078.

Send reprint requests to: Dr. María J. Garrido, Department of Pharmacy and Pharmaceutical Technology, Faculty of Pharmacy, University of Navarra, Apartado 177, Pamplona 31080, Spain. E-mail: mgarrido@unav.es